PORE STRUCTURE ANALYSIS OF COALS USING LOW FIELD NMR MEASUREMENTS AND THERMOGRAVIMETRY ANALYSIS

Benjamin Nicot[1], Serge Gautier[1], Marc Fleury[1] and Sevket Durucan[2]

[1] Institut Français du Pétrole, Rueil-Malmaison, France
[2] Imperial College London, United-Kingdom

This paper was prepared for presentation at the International Symposium of the Society of Core Analysts held in Trondheim, Norway 12-16 September, 2006

ABSTRACT

Four different coals were studied using a combination of T_2, T_1, FID and solid echoes measurements on saturated plugs and degassed cuttings. These measurements were performed on two NMR spectrometers working at a proton Larmor frequency of 2 and 23 MHz. The measurements on saturated plugs allow the characterization of the cleats, and the measurements on degassed cuttings allow the characterisation of the matrix. For the latter, thermogravimetry coupled with mass spectral analysis were also performed. The results indicate a coherent measurement of liquid protons from NMR and thermogravimetry when the FID decay is analysed using a combination of Gaussian and exponential functions. This allows the distinction between solid and liquid fractions and consequently an accurate estimation of the porosity of the samples. For the four types of coal studied, microporosity represents a significant fraction of the total porosity (from 0.41 up to 0.91) and can be grossly underestimated when using usual NMR petrophysical analysis.

INTRODUCTION

With the prospect of geological storage of CO_2, there is an increasing need for detailed characterisation of coal structure. Coals are generated by accumulation of dead plant debris and minerals such as clays, alumina or silica. Almost immediately after deposition and burial, biochemical and geochemical processes are initiated. With continued burial, these processes progressively cause coalification of the organic matter to form the maturational sequence of peat, brown coal, bituminous coal and finally anthracite (Tissot and Welte, 1978). These processes result in a very complex chemical composition and textural structure for coal. Coals typically have micro pores but also exhibit meso and macroporosity covering four decades in pore sizes.

Due to its complex nature, a variety of techniques have been used to determine the pore structure of coals and the problems well identified. For example, the adsorption of nitrogen at 77 K is a standard method used in determining the surface area of coal. However Anderson and co-workers (Anderson et al., 1965) have demonstrated that this approach underestimates coal surface areas. Indeed, activated surface diffusion limits the ability of nitrogen to access the micropores. Another routine experiment used to

characterise porous medium is the mercury porosimetry. Zwietering and van Krevelen (1954) used this technique to determine the pore size distribution of a coal. They noticed that the volume-pressure curve was linear between 7,500 and 1,5000 psia, which the authors attributed to sample compression. In addition, for these two methods, samples must be completely dry. This is questionable for samples having microporosity in the nanometre range, and for coal containing mineral such as clays. Hence, total drying of a coal could significantly modify the pore network leading to inaccurate measurements.

High field NMR has been used extensively to describe the chemical structure of coals (Botto, 1996). Low field NMR can be used to describe the pore structure of porous media and this is becoming an established measurement technique in petroleum geosciences. The main advantage is that the molecules saturating the porous media are used to probe the structure and therefore the drying problem is circumvented. Although NMR spin-lattice or spin-spin relaxation data are relatively easy to acquire, their detailed interpretation is often difficult when transforming relaxation times into pore size. This calibration requires a measure of the surface relaxivity which depends on a number of parameters (Glaves et al., 1988). In particular, it requires the determination of the specific surface area which must be measured with great care as discussed above. The pore shape also comes into account. Hayashi et al. (2001) used sorbed water NMR relaxation experiments to deduce that the pore shape is slitlike rather than cylindrical, as one would expect.

This paper focuses on the microporosity of coals which is not well described or quantified in the literature. This pore population may play an important role in the CO_2 storage processes (Shi and Durucan, 2003) and may be a significant fraction of the total porosity. In this research, the IUPAC pore size classification (1994) was adopted in defining the range of pore size distribution for micro (<20 Å), meso (20-500Å) and macroporosity (>500Å). The difficulty experienced in the use of NMR for microporosity analysis was that the NMR microporosity signal overlaps partially with the signal detected from the solid. Therefore, a methodology was developed to separate the solid and liquid signal contributions in order to quantify the microporosity. The NMR interpretation is supported by thermogravimetry and mass spectral analysis. This paper summarises the fundamentals of the NMR and thermogravimetry techniques used first, followed by the description of the standard relaxation measurements carried out on four different types of coals in order to calculate total porosity.

EXPERIMENTAL TECHNIQUES AND PROCEDURE

Coal samples

Large coal blocks from open cast or underground mine sites in the United Kingdom, France, Germany and Poland were collected for a variety of tests involving CO_2 storage research. Table 1 presents the relevant information on the origin and rank of the coals used in the study:

- the 9ft seam from the Selar open cast mine in South Wales, UK
- the Dora seam from the Rumeaux underground colliery in Loraine, France

- the Schwalbach seam from the Ensdorf underground colliery in Saarland, Germany
- seam 364 from the Brzesczce underground colliery in Upper Silesia, Poland.

From a given block of coal, two types of samples, hereafter referred as type A and type B, were prepared.

- Samples A are small pieces of about 5*5*5 mm in size. Prior to the measurements, these were oven dried for 24 hours at 80°C. These samples were used for matrix specific gravity measurements, NMR at 23 MHZ and for thermogravimetric analysis.
- Samples B are core plugs of 45 mm diameter and about 60 mm in length. They also were dried at 80°C for 24 hours, saturated with dodecane and then left several days at a pressure of about 30 bars. These were used for NMR analysis at 2 MHz. Dodecane, rather than water, was used as the saturating phase to avoid swelling or damaging the coal structure. Some tests performed with water have shown a desegregation of the coal in some cases.

Table 1: Coal characterisation data.

#	Coal Seam	Colliery	Volatile Matter (d.a.f.) %	Fixed Carbon Content (d.a.f.) %	Vitrinite Reflectance (%)	Rank Description	Specific Gravity
1	9 ft	Selar	9.50	90.40	2.41	Anthracite	1.35
2	Dora	Rumeaux	16.50	83.50	0.71	Semi-anthracite	1.50
3	Schwalbach	Ensdorf	41.21	56.40	0.79	High Volatile Bituminous	1.71
4	Seam 364	Brzesczce	-	-	0.77	High Volatile Bituminous	1.38

The specific gravity measurements were made with a Micromeritics helium picnometer. The values reported in Table 1 are the average over five consecutive measurements. The other data listed in this table were not measured on the samples described here. The samples represent a large variation of density ranging from 1.35 up to 1.71. The coring of plugs from type A1 coal (smallest density) was very difficult due to the fragility of the coal.

NMR techniques

The two low field NMR instruments used were the Maran-Ultra from Oxford Instruments. For the analysis of the small samples (type A), a 23 MHz tool equipped with an 18 mm probe was used (total dead time of 12 μs). The inter-echo time τ of the CPMG sequence described below was 35 μs. Due to its short dead time, this tool allows the observation of solid echoes.

For the larger plug samples (type B), a 2.2 MHz tool equipped with a 50 mm probe was used (total dead time of 45 μs). The inter-echo time τ of the CPMG sequence was 55 μs.

CPMG and Inversion Recovery pulse sequences

The magnetisation decay measured during a CPMG or inversion recovery experiment (Figure 1) was fitted to a discrete multi-exponential decay of the form:

$$M_{XY}(2n\tau)/M_0 = \sum_i A_i \exp\left(-2n\tau/T_{2i}\right) \quad (1)$$

$$\frac{1}{2}(1 - M_Z(\tau)/M_0) = \sum_i A_i \exp\left(-\tau/T_{1i}\right) \quad (2)$$

where T_{2i} or T_{1i} are predetermined sets of values spaced logarithmically. To increase the resolution of short relaxation times, the magnetization amplitude after the P90 pulse (Figure 1) can be added to the data set in (1). This data set will be referred to as the FID-CPMG. The calculation of the amplitudes A_i from the measured signal is a well known ill-posed problem and a regularisation method must be used to avoid oscillations of the solution (Tikhonov and Arsenin, 1977). In the software used, the following error function is minimised:

$$\chi^2 = \sum_j \left(M(t_j) - \sum_{i=1}^{m} A_i \exp\left(-t_j/T_{2i}\right) \right)^2 + \alpha^2 \sum_{i=1}^{m} A_i^2 \quad (3)$$

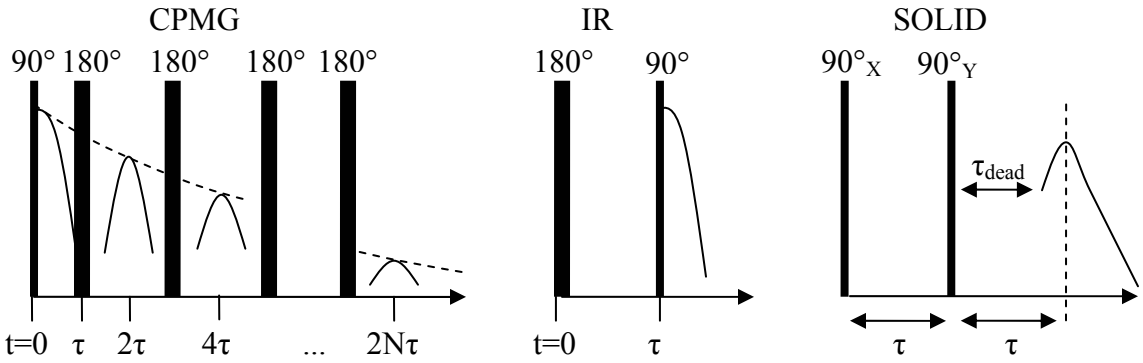

Figure 1: CPMG and IR (inversion recovery) sequences used to measure the transverse and longitudinal relaxation time distribution. The solid echo sequence is also presented.

The top of the echoes were used to calculate the magnetisation decay M(t). where α is the regularisation coefficient and t_j is a set of time interval spaced logarithmically. The choice of the optimum α is somewhat arbitrary. It is chosen as the highest value at which the lowest χ^2 value is obtained. When different distributions are compared, a unique value of α is imposed.

Solid Echo pulse sequence

Ordered dipolar interactions can be refocused using the solid echo pulse sequence (Callaghan, 1991). Figure 1 presents the pulse diagram used in the experiments described here. In order to visualise echo formation the condition $\tau_{dead}<\tau$ must be achieved. This is only possible for dead times of the order of 10 μs because the solid echo is not observed for τ larger than about 30 μs. The large probe diameter of the 2 MHz apparatus does not allow this type of measurement. Therefore, they have been performed only on the 23 MHz apparatus.

Thermogravimetric analysis

The thermogravimetric analysis (TGA) experiments were carried out on a Mettler TGA851. Approximately 50 mg of coal sample was placed in platinum crucibles and heated from room temperature to 800°C with a ramp of 10°C/min, under 25 mL/min helium flow. The temperature and sample weight were continuously recorded. A Pfeiffer Thermostar quadrupolar mass spectrometer directly coupled to the balance allows recording the evolution of the emitted gas composition from the samples during the heating process. The experiments were performed on samples of type A.

RESULTS AND DISCUSSION

Sample type A

NMR results

Coals are made of an organic matrix containing hydrogen atoms. As these protons are part of the solid, their NMR relaxation time is very short. Similarly, water in micropores lead to very short relaxation times. Therefore, there is the potential to confuse these two types of protons. Fortunately, the theoretical magnetisation decay functions are different and the distinction between solid and high mobility (liquid) protons can be made. All the experiments presented in this section were performed on samples of type A at 23 MHz. Dry samples with no water present in the meso and macro porosity were used. However, there still was a significant amount of liquid in the microporosity, as discussed below.

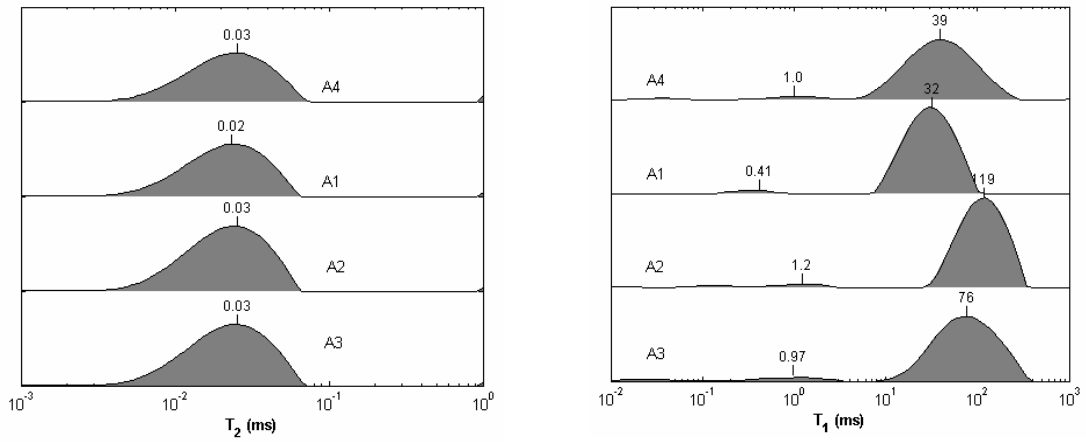

Figure 2: T_2 and T_1 relaxation time distribution at 23 MHz for sample type A.

The microporosity was first studied using T_1 and T_2 measurements (Figure 2). For T_2, the FID-CPMG sequence was used. For all types of coal, very short T_2 values around 20 μs were observed. Note that the mode of the T_2 distribution is at the limit of the relaxation time resolution and that components smaller than 20 μs are due to the regularisation procedure used in the multi-exponential analysis. On the other hand, the T_1 distributions indicate much longer relaxation times (above 30 ms) with a small fraction of protons relaxing at about 1 ms. The population with the highest T_1/T_2 ratio could be attributed to solid protons, whereas other protons could be interpreted as liquid. This simple experiment was the first evidence for the existence of both liquid and solid state protons in coals.

The solid echo sequence was used to identify the solid protons. Due to the solid state dipolar interactions, an echo is formed after two 90° pulses whereas in the liquid state this is not observed. An example of such an echo is presented in for sample A3. At high field (300 MHz) Kuratnik et al (1992) performed experiments on natural coals and found the typical signature of solid interactions: a Gaussian spectral line shape in contrast with the Lorentzian shape associated with the liquid state. The Gaussian shape arises from ordered interactions and represents a form of inhomogeneous broadening. This can be refocused using the right pulse sequence. At low field, the frequency spectrum is dominated by the field inhomogeneities and the spectral shape is difficult to observe. When setting $\tau > \tau_{dead}$, the solid echo technique allows one to identify the protons forming the echo, later referred as solid protons, and the protons generating the exponential decay (Figure 3) roughly appearing after 0.03ms. The liquid contribution is small compared to the solid but not negligible compared to the porosity found in the meso and macropores described later. Therefore, in order to estimate the amount of liquid, one could consider only the data after 0.03 ms. However, it was found out that the fitting was too sensitive to the choice of the cut-off. This method would require an analytical function for the solid echo shape.

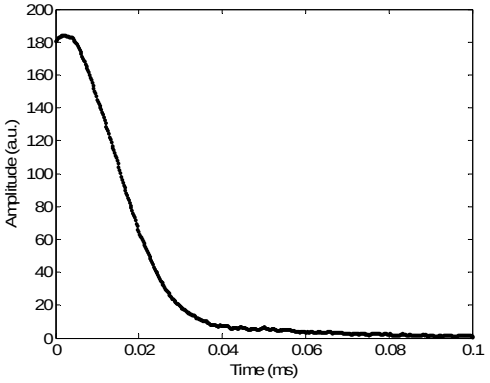

Figure 3: Solid echo observed on sample A3. Acquisition parameters: τ=15µs and τ_{dead}=12µs

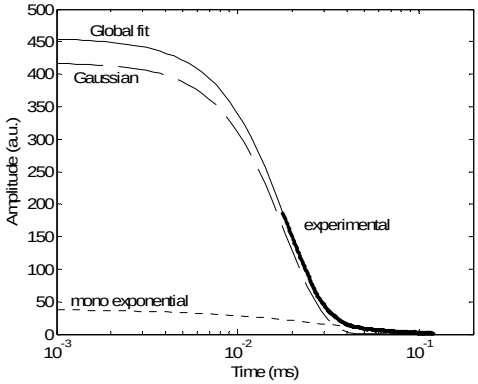

Figure 4: Experimental FID acquired on sample A3. FID is fitted by a sum of a Gaussian and an exponential function

A simpler approach consists in studying the FID time dependence, as performed by the food industry to separate low and high mobility protons. The standard method used by this industry is to compare FID intensities at 11 and 70 µs after the 90° pulse in order to determine a solid-liquid fraction (IUPAC, 1982). In the case of coal, however, the transverse relaxation time of the liquid fraction is very small. As can be seen in Figure 4, the amplitude at 70 µs is not representative of the liquid amplitude. To circumvent the problem of choosing a point, it was decided to fit the FID curve and extrapolate at zero time to obtain solid-liquid fraction.

As described before, solid protons lead to a Gaussian spectral line shape. The Fourier transform of a Gaussian being a Gaussian, the FID exhibits a Gaussian shape in the time domain too. Therefore, the FID curve M(t) can be considered as the sum of a solid (Gaussian) contribution and a liquid (exponential) contribution (Figure 4) defined by :

$$M(t) = A_G G(t) + A_E E(t) \quad (4)$$

where

$$G(t) = exp\left(-\frac{t^2}{2\sigma^2}\right) \quad (5)$$

$$E(t) = \exp\left(-\frac{t}{T_2}\right) \quad (6)$$

The parameters A_G, A_E, σ and T_2 are obtained from least squares optimisation. To transform A_G and A_E into volumes, one must use reference samples with known volumes and hydrogen index. For the liquid fraction, water was used. No attempt was made to calibrate the solid fraction. For practical convenience, all the liquid calibrations were made relative to the mass and not volume, thus the solid density was needed. As there is very little water remaining in the microporosity, the measured (total) density of the

sample was used as the density of the solid matrix. This procedure was applied to the analysis of porosity in the four coals studied and the results are presented in Table 2.

Thermogravimetric results

To confirm the findings of the NMR analysis described above, thermogravimetry experiments were performed on the same coals (type A). The weight loss with increasing temperature for each type of coal (Figure 5) gives an indication of the presence of liquids. In addition, the mass spectrometer analyser provides a qualitative analysis of the composition of gases released. Figure 6 presents the data on the release of water, methane and CO_2 with increased temperature. These graphs are presented using arbitrary scales. However, it should be noted that the volume of CO_2 is relatively small compared to the volume of water and methane.

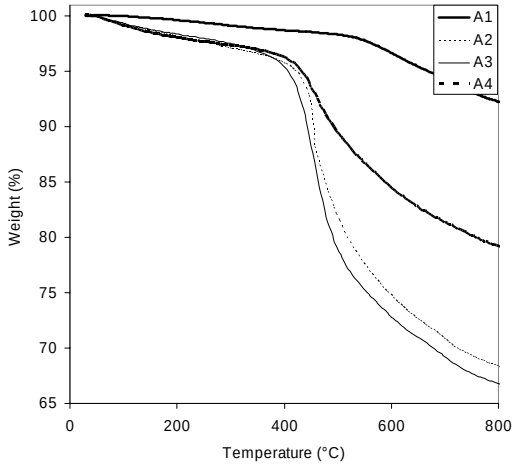

Figure 5: Weight loss during the thermogravimetry experiments.

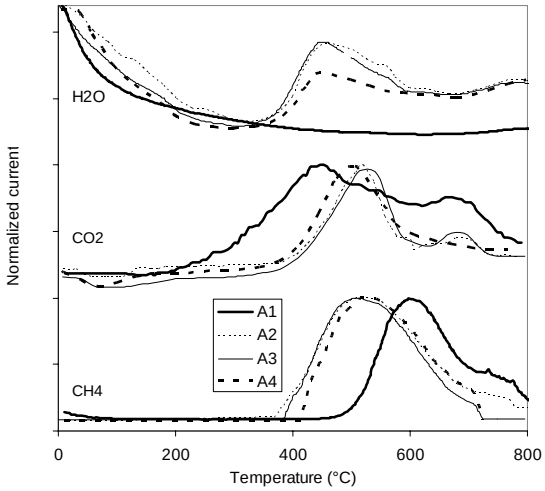

Figure 6: Mass spectroscopy performed simultaneously with thermogravimetry.

The results clearly show two domains for the temperature range. In the first one, between room temperature and 300°C, the weight loss is only due to water and the rate of change with temperature is small. This water release is either due to evaporation of the moisture included in the microporosity, or/and due to the dehydration of minerals such as clays or alumina. The second domain concerns the high temperature range between 300 to 800°C. In this range, increase of weight loss is significant. This is due to the release of methane, carbon dioxide and, for some coals, water. Methane release could be attributed to thermal cracking of alkyl chains of coal. The CO_2 is due to combustion of coal, the oxygen source necessary for combustion is the coal itself. It must be noted that, as the detected current of mass spectrometer has been normalized with respect to the maximum value for the clarity of the graphs, it is not obvious in the graphs that the CO_2 production for sample A1 is much smaller compared to that of the other samples. The high temperature water can be attributed to:

- combustion,
- minerals dehydroxylation (modification of structural properties under temperature),
- thermal cracking of hydroxyl groups of coal.

No matter what the origin of high temperature water may be, this has no direct relationship with microporosity as this water is due to the "solid state" protons.

Table 2: Microporosity of coals from NMR and thermogravimetry (TGA).

Samples	% water from NMR	% water from TGA
A1	0.7	1.4
A2	6.7	4.7
A3	7.9	4.3
A4	3.8	3.9

The mass losses determined from thermogravimetry using a cut-off at 300°C are comparable to the microporosity fraction determined from NMR. However, NMR overestimated the microporosity fraction for samples A3 and A2. It should be noted that only a tenth of mg of the NMR sample was used for thermogravimetry measurements and that this may be a possible explanation of the discrepancy observed for these samples.

Sample type B

These samples were characterised using standard NMR petrophysical methods on plugs, except that dodecane was used as the saturating fluid, and not water as it s usually the case. First, a T_2 experiment allows the determination of the pore volume after comparing the magnetisation intensity M(t=0) with a know volume of the saturating fluid. The porosity of the sample is then obtained by combining this measurement with the solid volume measurement. Afterwards, the so-called pore size distribution is obtained from the relaxation time distribution:

$$\frac{1}{T_2} = \frac{1}{T_{2B}} + \rho_2 \frac{S}{V} \qquad (7)$$

where T_2 is a component of the distribution, S/V is the surface to volume ratio of a class of pores, ρ_2 is the surface relaxivity and T_{2B} is the bulk relaxation time of the saturating fluid (for dodecane $T_{2B} \cong 1000$ ms).

The above relationship (Eq. 7) is true in the fast diffusion regime (Godefroy et al., 2001) and neglecting the effect of internal gradient. The surface relaxivity ρ_2 is needed to transform relaxation times into pore sizes but this is usually not performed because ρ_2 is difficult to measure. It depends on the surface properties (in particular paramagnetic impurities) and the fluid. Glaves et al. (1988) found that the water surface relaxivity is of the order of 0.1 μm/s; Dodecane molecules are much bigger than water and therefore the surface relaxivity for dodecane is expected to be smaller than the water surface relaxivity. Assuming $\rho_2 \approx 0.1$ μm/s, a slitlike pore shape and a lower measurement limit of 0.1 ms for T_2, it is found that the lowest resolved pore size is of the order of 0.1 nm, and the largest size is of the order of 0.1 μm or less. Above 0.1 μm, the intensities will accumulate at the bulk T_2 value (1s for dodecane) and will not be lost in the pore volume determination.

The relaxation time distributions measured on the B type samples saturated with dodecane (Figure 7) cover the entire measurable range (0.1 up to 1000 ms). For all coals,

two and sometimes three distinct populations were recognised, confirming the previous observations made by Glaves *et al*. (1988). The microporosity is represented by T_2 values smaller than 1 ms and the meso and macro porosity is represented by T_2 values above 1 ms. A distinction between meso and macro porosity representing the cleat network could be made. For samples B3 and B4 there is a continuum of sizes extending over more than 1 decade not suggesting a clear separation between these two populations (Figure 7).

However, the measured relaxation times characterising the microporosity are at the limit of T_2 resolution (τ=55 μs). Hence, neither T_2 times nor microporosity fractions are correctly estimated by CPMG as discussed below.

When comparing the 2 and 23 MHz results (Figure 2 and Figure 7), there is an apparent contradiction between the typical relaxation times characterising the microporosity (0.03 ms at 23 MHz and 0.1 ms at 2 MHz). In fact, the characterisation of the microporosity components is highly dependent on the value of the inter-echo time 2τ as shown in Figure 8. At 23 MHz, short relaxation times can be detected due to short inter-echo times and the capability of acquiring the magnetisation after the P90 pulse (t=12 μs). The magnetisation decay is then acquired at time t=12, 70, 140, $2n\tau$ μs. Under these conditions, a high amplitude peak at about 20 μs was detected (Figure 8). When the magnetisation after the P90 pulse is removed from the data set, the mode of the microporosity distribution is shifted to 70 μs. When the magnetization signal is re-sampled using a τ value of 2x50 μs to mimic the 2 MHz apparatus, the mode of the distribution is further shifted to 100 μs and the amplitude severely reduced. The conclusion is that a standard large diameter 2 MHz spectrometer cannot characterise accurately the microporosity but is well suited to characterise large samples in which the cleat network is still present.

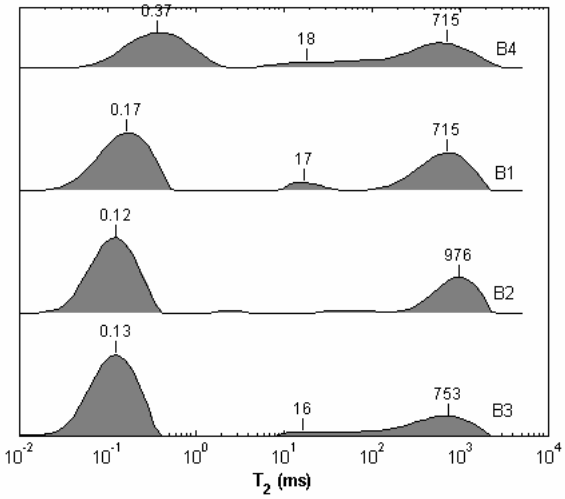

Figure 7: T_2 relaxation time distribution at 2 MHz for sample type B. The limit of resolution is about T_2=0.1 ms. Shorter components are due to the regularisation procedure.

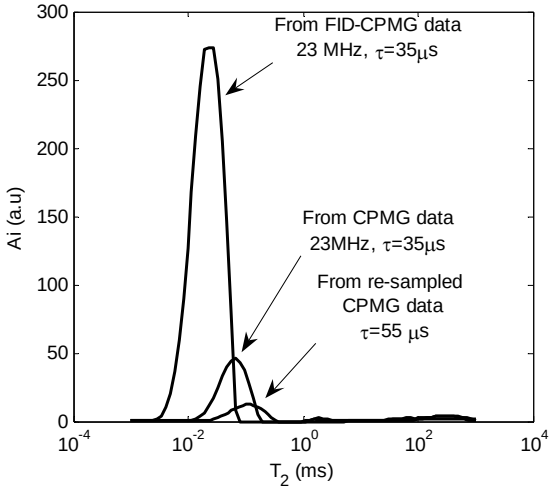

Figure 8: Effect of increasing inter-echo time on the microporosity characterisation. The magnetisation decay is the same for the 3 cases. The distribution obtained from re-sampled CMPG data is representative of measurements performed at 2 MHz.

It was also observed that the microporosity modes did not vary before and after saturation by dodecane. When comparing the mass deduced from the NMR distributions excluding microporosity (T_2>2 ms), with the mass difference before and after saturation (Figure 9), a very good correlation between these two quantities was observed. Dodecane did not penetrate into the microporosity which was already filled with water. The samples of type A have also displayed the same behaviour.

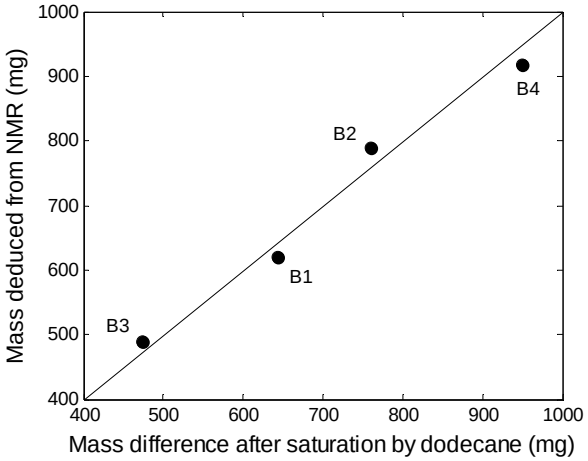

Figure 9: Comparison of the mass after saturation by dodecane and the mass deduced from the NMR measurements for relaxation times larger than 2 ms (meso and macro porosity, type A samples). The dodecane did not penetrate into the microporosity.

Total porosity

The total porosity of the coal is the sum of the microporosity obtained from type A using the FID analysis and the porosity obtained from larger type B samples using CPMG (Table 3), the latter representing essentially the cleat network. The results indicate that the microporosity represent an equal or a much larger fraction of the total porosity.

Table 3: Total porosity for all coal types using a combination of measurements on degassed samples and dodecane saturated samples.

#	Origin	Microporosity (%)	Porosity (meso+macro) (%)	Total porosity (%)
1	South Wales, UK	0.7	1.0	1.7
2	Lorraine, France	6.7	1.2	7.9
3	Saarland, Germany	7.9	0.8	8.7
4	Upper Silesia, Poland.	3.8	1.5	5.3

CONCLUSION

Four different coals of different origin were studied using low field NMR. T_2 NMR relaxation is well suited to characterise coal structure because it has a large dynamic range spanning over more than four decades in pore sizes, but it has some limitations. In this research, the cleat network of coal (macro and meso porosity) was characterised using measurements performed at 2 MHz on dodecane saturated plugs.

Microporosity was characterised using measurements at 23 MHz on smaller degassed coal pieces. It was established that the CPMG technique does not provide a satisfactory description of the relaxation time and amplitude of the micropore signal. The T_1 relaxation data and the solid echo technique used have shown that two populations of solid and liquid state protons exist in coal, both having very short T_2 relaxation times. In practice, it is proposed to use the FID to separate solid from liquid state protons and decompose this curve into a sum of Gaussian and exponential functions. Using thermogravimetry and mass spectroscopy, the presence of liquid water was studied in the same coal samples. The microporosity volumes of liquid determined from FID analysis and thermogravimetry were found to be comparable, confirming the robustness of the techniques proposed in this research.

Finally microporosity represents a significant fraction of the total porosity for the four types of coal studied (from 0.41 up to 0.91) and can be grossly underestimated when using usual NMR petrophysical analysis.

ACKNOWLEDGMENTS

This research was carried out as part of a European Commission "Network of Excellence on Geological Storage of CO_2 (CO2GeoNet)", Contract No SES6-CT-2004-502816, 2004-09. The authors also wish to thank Dan Bossie-Codreanu, who provided some of the coal samples and B. Rebours and F. Filali who performed the thermogravimetry measurements reported in this paper.

REFERENCES

Anderson R.B., Bayer J, Hofer LJE. Fuel, 44: 443, 1965.

Botto E.R. Encyclopedia of Nuclear Magnetic Resonance, Ed. John Wiley and sons, 1996.

Callaghan P.T. Principle of Nuclear Magnetic Resonance Microscopy. Oxford Science Publication, 1991.

Glaves L.G., Davis P.J., Gallegos D.P., Smith D.M., Energy and Fuel, 2: 662, 1988.

Godefroy S., Korb J.P., Fleury M., Bryant R.G., Surface nuclear magnetic relaxation and dynamics of water and oil in macroporous media. Physical Review E, 64, 2001.

Hayashi J., Norinaga K., Kudo N., Chiba T., Energy Fuel, 15: 903, 2001.

International Union of Pure and Applied Chemistry, Pure Appl Chem, 66:1739, 1994.

IUPAC. Standard Methods for the Analysis of Oils, Fats and Derivatives, 6th edn., 1st Supplement, Part 6. Oxford: Pergamon Press, 1982.

Kuratnik V.V., Denisov V.P., Smirovna G.G., Revokatov O.P., Lomonosov M.V. Nuclear Magnetic Resonance Investigation of adsorption of methane on natural coal. Russian Journal of Physical Chemistry, 66: 10, 1992.

Tissot B.P., Welte DH. Petroleum Formation and Occurrence, ed. Springer-Verlag Berlin Heidelberg New York, 1978.

Tikhonov A.N., V.Y. Arsenin, Solution of Ill-Posed Problems, Winston and Son, Washington DC, 1977.

Shi J.Q. , S. Durucan, A bidisperse pore diffusion model for methane displacement desorption in coal by CO2 injection, Fuel, 82, 1219-1229, 2003.

Zwietering P., Van Krevelen D.W., Fuel, 33: 331, 1954.